Fermilab Library
0 1160 0026429 5

DPNU-93-40

DPNU - 93 - 40

# RECENT RESULTS FROM TRISTAN AT KEK

Shiro Suzuki
Dept. of Physics, Nagoya University
Furo-cho, Chikusa-ku, Nagoya 464-01, Japan

DEC 29 1993

ABSTRACT

Recent results of TRISTAN experiment with high luminosity run are reviewed.

Updated results on lepton and quark pair production in the annihilatiopn processes are presented, and limits on the compositeness scale and lower mass limit for extra $Z$ boson are given. Total hadronic cross section is presented in the effective Born approxiamtion. A search for a resonance suggested by L3 group is done in several different final states. Strong coupling $\alpha_s$ is derived from several observables with improved theoretical framework. Running nature of $\alpha_s$ is studied in comparison with PEP4 and ALEPH data. Different property of quark and gluon jet is examined. Hard scattering of two photons are established and the data provide information on quark and gluon distribution in the photon.

Talk presented at the XXI SLAC Summer Institute on Particle Physics, Stanford, California, July 26 - August 6, 1993

## 1 Introduction

TRISTAN was comissioned in late 1986. It started up at the center of mass energy of 50 GeV, and gradually ramped up to 64 GeV. Since 1990, after SLC and LEP started operation at around 90 GeV, we set our operation energy at 58 GeV, where we can expect high luminosity with much stable opearting condition. This is also the energy region where we can observe large interference effect of virtual photon and $Z^0$. After QCS insertion, current typical integrated luminosity per day reaches to $800nb^{-1}$. Our goal is to collect $300pb^{-1}$ in 2 years, and move to TRISTAN-II, i.e. KEK asymmetric B-factory. Since the machine has been operated quite nicely for this one and a half years (fig. 1), we are quite confident of achieving this value.

This report is based on the analysis work with the data sample of about $100 \sim 150pb^{-1}$ .

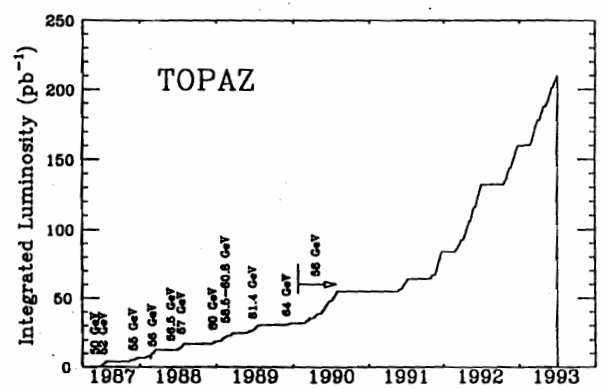


Figure 1: Accumulated integrated luminosity since 1987.

## 2 Electroweak Processes

First we present the updated results in the basic annihilation processes in the interference regin of $\gamma^*$ and $Z^0$.

Table 1: Total cross section and forward-backward asymmetry of lepton pair production by three groups. Errors are quoted in the order of statistics and systematics.

| | | $\sqrt{s}$ GeV | $\mu^+\mu^-$ | $\tau^+\tau^-$ | S.M. |
|---|---|---|---|---|---|
| R | TOPAZ | 57.9 | $0.99 \pm 0.03 \pm 0.05$ | $1.06 \pm 0.03 \pm 0.05$ | 1.053 |
| | VENUS | 58.0 | $0.98 \pm 0.02 \pm 0.03$ | $0.99 \pm 0.03 \pm 0.03$ | 1.054 |
| | AMY | 58.0 | $0.96 \pm 0.03 \pm 0.03$ | $1.02 \pm 0.03 \pm 0.03$ | 1.054 |
| A | TOPAZ | 57.9 | $-0.312 \pm 0.025 \pm 0.011$ | $-0.313 \pm 0.039 \pm 0.010$ | $-0.334$ |
| | VENUS | 58.0 | $-0.320 \pm 0.020$ | $-0.300 \pm 0.030$ | $-0.338$ |
| | AMY | 58.0 | $-0.342 \pm 0.024 \pm 0.007$ | $-0.337 \pm 0.028 \pm 0.014$ | $-0.338$ |

## 2.1 Lepton pair production

The total cross section and forward-backward asymmetry of lepton pair production reported from three groups are summarized in table 1. Still we have somewhat lower cross section in $\mu^+\mu^-$ and $\tau^+\tau^-$ pair production than the standard model expectation, but with not much significance. On the other hand, asymmetry shows good agreement with the standard model. Overall agreement of TRISTAN average data with the standard model is good (fig. 2).

Because the data are consistent with the standard model, we can place several limits from its deviation. TRISTAN is in better position than SLC/LEP for setting compositeness limit because there is no amplitude saturation by $Z^0$. From the angular distribution, we can set limit of the compositeness parameter $\Lambda$ as in table 2. They now exceed the previous TRISTAN, PEP and PETRA experiments.[1]

TRISTAN is also in a good position of looking for extra Z bosons ($Z'$). With high precision data, we can look for contribution from $Z'$ which interferes with $Z^0$. Fig. 3 shows a sensitivity of our measurement to the various types of $Z'$, assuming $M_{Z'}$ =150 GeV and no mixing. From these data plus hadronic data from TOPAZ experiment,[2] and also combining data from other TRISTAN experiments,[3,4] we summarise the 95% C.L. mass limits of extra Z bosons[5] associated with $E_6$ extensions of the standard model(table 3), which are compared with the value from



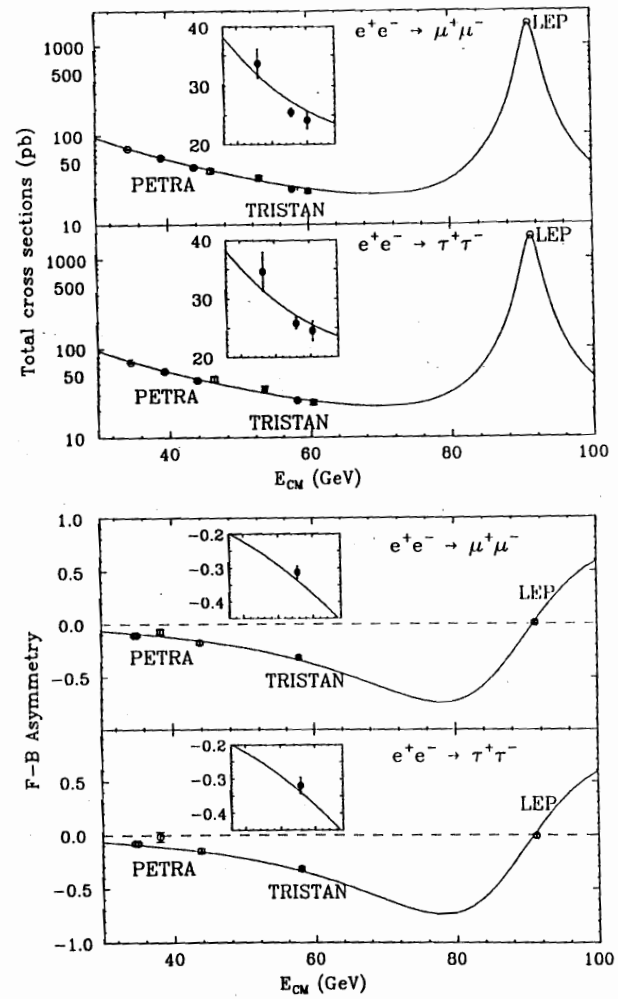


Figure 2: TRISTAN average of total cross section and forward-backward asymmetry of lepton pair production. Data from PETRA and LEP are also plotted for comparison.

Table 2: Limits on the compositeness scale in TeV at the 95% confidence level.

| $\Lambda^+/\Lambda^-$(TeV) | $e^+e^- \to \mu^+\mu^-$ | $e^+e^- \to \tau^+\tau^-$ | $e^+e^- \to l^+l^-$ |
|---|---|---|---|
| RR coupling | > 2.1/3.1 | > 1.8/2.7 | > 2.2/4.1 |
| LL | > 2.1/3.0 | > 1.7/2.6 | > 2.2/3.9 |
| VV | > 11.2/3.4 | > 3.5/4.3 | > 7.1/4.2 |
| AA | > 3.1/7.0 | > 2.7/3.9 | > 3.2/8.7 |

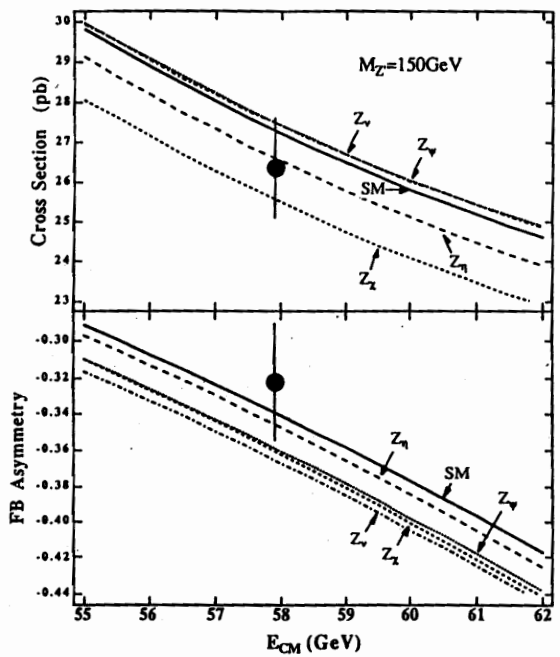


Figure 3: Sesitivity of lepton pair measurements to the existence of various $Z'$s as a function of $E_{CM}$, where $M_{Z'}$=150GeV is assumed with no $Z' - Z^0$ mixing. The data points are from TOPAZ with $\mu$ and $\tau$ combined.



Table 3: The 95% C.L. lower limits for various $Z'$s with a comparison to $p\bar{p}$ data.

| $M_{Z'}$ limit (GeV) | $Z_1$ | $Z_\psi$ | $Z_\chi$ | $Z_\eta$ | $Z\nu$ |
|---|---|---|---|---|---|
| TOPAZ | > 290 | > 146 | > 134 | > 100 | > 164 |
| TRISTAN all | > 430 | > 166 | > 245 | > 145 | > 196 |
| CDF($p\bar{p}$ ) | > 412 | > 320 | > 340 | > 340 | -- |

CDF collaboration.[6]

## 2.2 Total hadronic cross section

Our traditional way of presenting $R_{had}$ data was to derive 'tree level' cross section by making electroweak radiative correction up to 2nd order. With that method we were not free from a few % uncertainty in the higher order correction ('short distance effect'), for instance, the effect of unknown parameters such as $M_{top}$ and $M_{higgs}$. Also a big problem was that the presented 'experimantal' data could not simply be compared with others if different correction models were taken.

New method which have been adopted by LEP group is only to make QED correction up to 2nd order, which can be calculated accurately, and leave other 'short distance' correction untouched ('effective Born' approximation). Effective cross section by this correction scheme, which is free from higher order ambiguity, is to be compared with theoretical calculation in which all 'short distance' phenomena are included. Then the definition of corrected experimental data will not be changed group by group, since $1 + \delta_{QED}$ is well defined quantity. Another merit of taking this method for us is capability of direct comparison with the LEP data. We used the KORALZ program[7] to calculate the radiative corrections up to $O(\alpha^2)$ with exponentiation of leading logarithm effect. TOPAZ data is shown in fig.4 utilising this correction scheme. Highest statistics data at 58 GeV gives $\sigma^{eff} = 143.8 \pm 1.5\ (stat.) \pm 5.4\ (sys.)\ pb$ for an integrated luminosity of $85.5pb^{-1}$. This is a good agreement with the expectation value of $142.0pb$ for the S.M. with $M_Z$=91.13GeV, $M_{top}$=150GeV and $M_{higgs}$=100GeV.

In the S.M. framework, we can determine the running QED coupling $\alpha$. The gotten value $\alpha_{eff}^{-1} = 128.6 \pm 2.6$ at $Q^2 = 58^2\text{GeV}^2$ also agrees well with the expectation of 129.8 from the S.M.

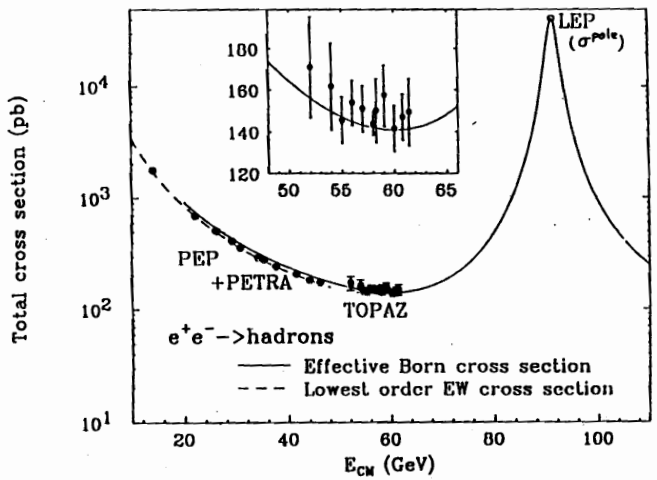


Figure 4: Comparison of the total hadronic cross section with effective Born cross section and lowest order EW cross section of the standard model.

## 2.3 D* production

Forward-backward asymmety of charm pair productin was measured by detecting fast going $D^*$ in the jets.

One method is to look for mass difference $\Delta M = M_D^* - M_D$, which gives very sharp peak due to small Q-value of $D^* \to D\pi$ decay. $\Delta M$ for several different $D$ final states are shown in fig. 5(a)-(c). Combination of (a)-(c) is shown in fig. 5(d), where the histogram underneath is estimated background. Angular distribution thus determined is compared with the standard model (fig. 6). Asymmetry $A_{c\bar{c}}$ is $-0.57 \pm 0.22 \pm 0.05$ by VENUS[8] and $-0.50^{+0.33}_{-0.29} \pm 0.08$ by TOPAZ.[9]

Another method is to detect inclusive soft $\pi$ from $D^*$ decay. Small Q-value gives very sharp peak at low $p_t$ distribution, 40 MeV/c at most, with respect to the jet axis (see fig. 7). By this method, we got $A_{FB} = -0.49 \pm 0.15 \pm 0.08$ from TOPAZ,[9] $-0.73^{+0.22}_{-0.30}$ from VENUS[8] and $-0.67 \pm 0.20$ from AMY.[10]

Results combining above measurement, $c\bar{c}$ asymmetry are plotted in fig. 8 together with the results from other laboratories with different center of mass energies. This shows overall good agreement with the S.M.

Also $b\bar{b}$ asymmetry is shown in fig.9 for reference.



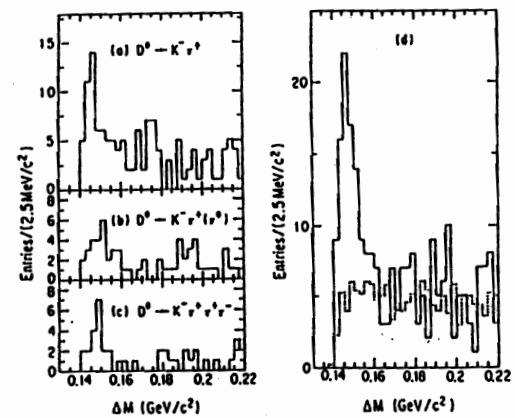


Figure 5: Mass difference $\Delta M = M_D^* - M_D$ measured by VENUS collaboration for $D^{*\pm} \to \pi_s^\pm D^0(\overline{D^0})$ following $D^0(\overline{D^0}) \to K^\mp\pi^\pm$ (a), $K^\mp\pi^\pm\pi^0$ (b) and $K^\mp\pi^\pm\pi^\pm\pi^\mp$ (c). Combined result is shown in (d). The dotted line underneath is estimated background.

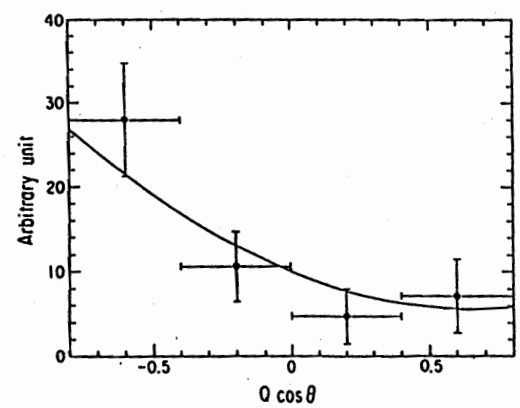


Figure 6: Angular distribution of charm quark pair production measured by $D^{*\pm}$s with the $\Delta M = M_D^* - M_D$ method (VENUS).

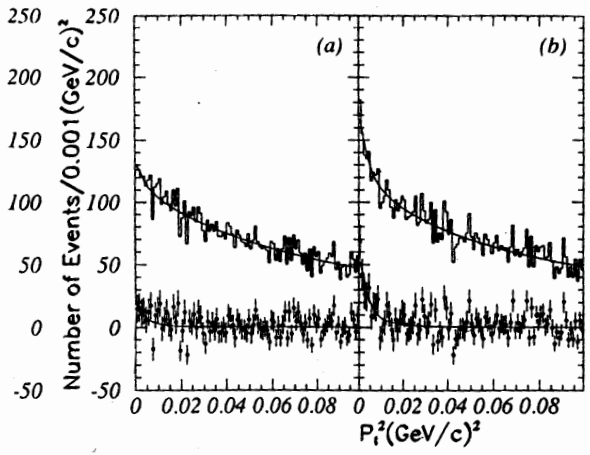


Figure 7: $p_t^2$ distributions of $\pi^{\pm}$s in (a) forward and (b) backward angular regions. Dots are the experimental data after subtracting estimated backgrounds.

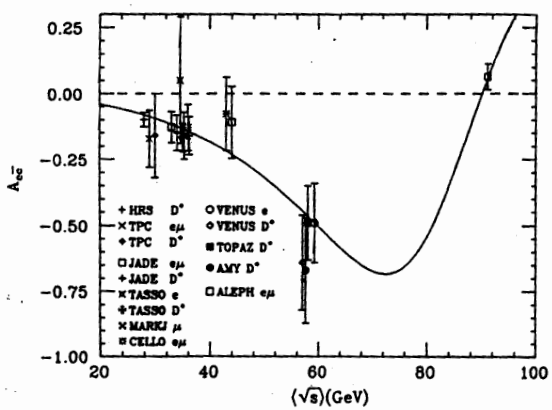


Figure 8: $A_{c\bar{c}}$ by various measurement methods and experimental groups. Curve presents the prediction of the standard model.



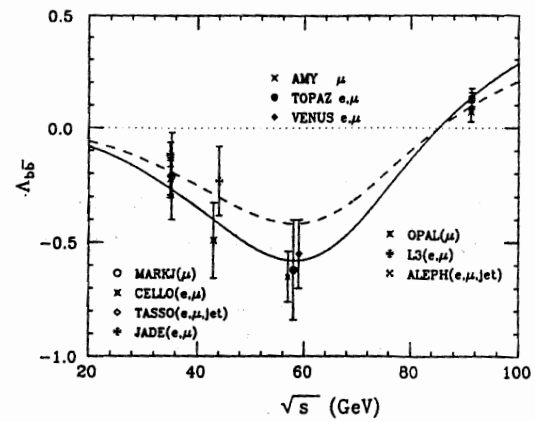


Figure 9: Summary of $A_{b\bar{b}}$ by various groups and labs. The solid curve shows the standard model with no $B\bar{B}$ mixing, and the dashed curve shows the case with $\chi_d = 0.17$ and $\chi_s = 0.5$.

## 3 Search for a resonance

Last year, excess of $\gamma\gamma$ distribution around 59 GeV in $l^+l^-\gamma\gamma$ events was reported by L3 group.[11] This excess could be a non-higgs like particle with mass 59GeV/c$^2$, which has large branching fraction to $\gamma\gamma$ final state and spin 0 or 2 or more (scalar or tensor). If it is a new boson '$X$' couples to $e^+e^-$, we could be very much sensitive to this state even if its total width is very narrow. We carried out energy scan to search for $X$ in the final states of $\gamma\gamma$, $e^+e^-$, $\mu^+\mu^-$ and hadrons in the energy range of 58 to 60 GeV with 250MeV step, with integrated luminosity of more than $1pb^{-1}$ at each scan point. Since the energy spread of TRISTAN beam is about 100MeV in $\sigma$, the sensitivity is continuous with energy and has no gaps in this energy range.

Fig.10 shows the results from VENUS[12] and AMY[13] for $\gamma\gamma$ and $e^+e^-$ final states. Solid lines are the S.M. prediction, and dotted or dashed lines are with hypothetical resonance with small coupling. AMY results gives smaller $\chi^2$ with a resonance, but with less significance. TOPAZ results for several final states[14] are shown in fig.11(a). VENUS, AMY and TOPAZ data do not show discrepancies from the S.M. prediction.

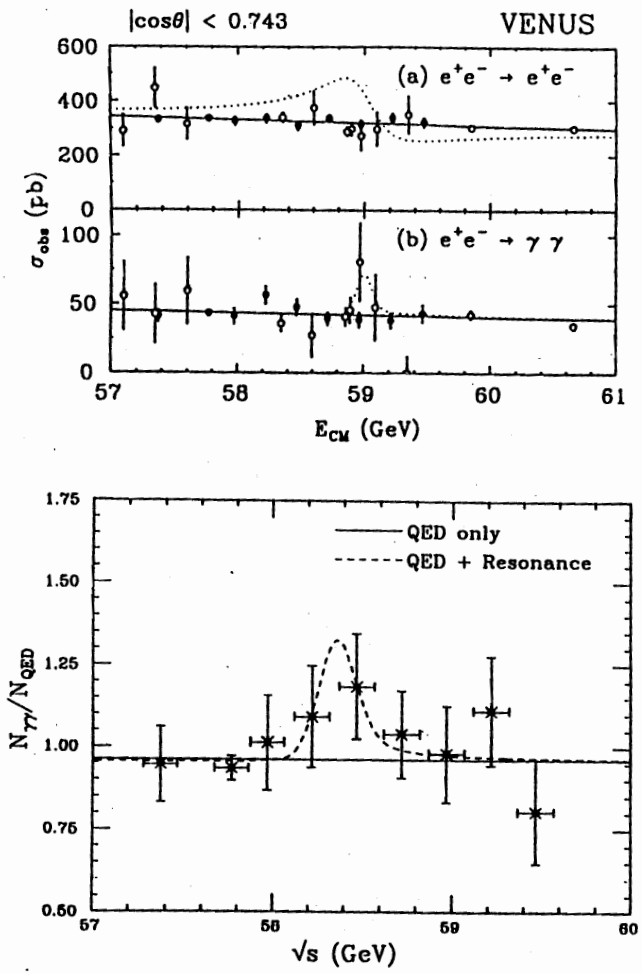


Figure 10: Scan results by VENUS (top fig.) and AMY (bottom fig.).



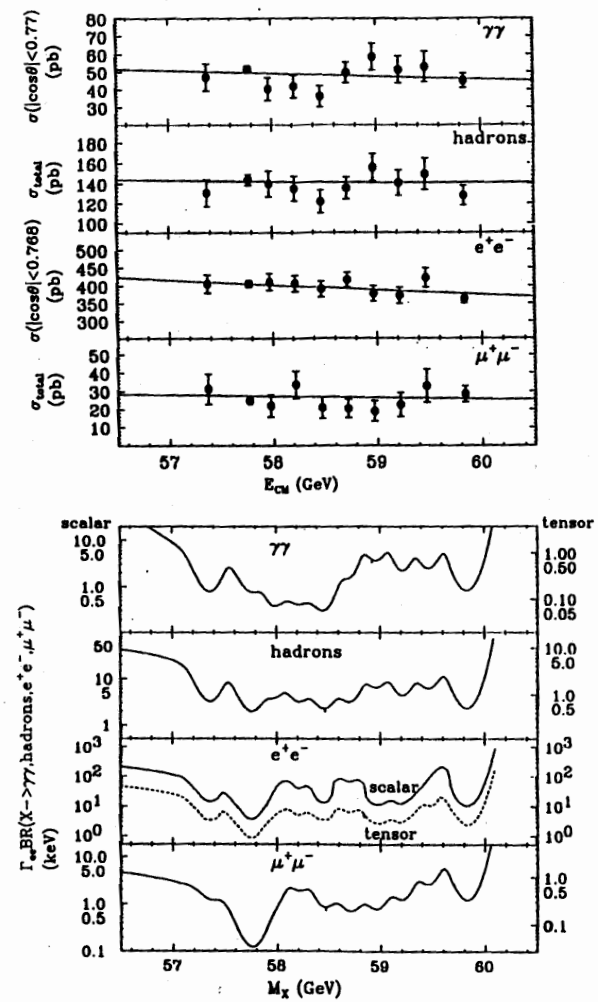


Figure 11: (a) Scan results of TOPAZ in the final states of $\gamma\gamma$, hadrons, $e^+e^-$ and $\mu^+\mu^-$, and (b) 95% C.L. upper limit of $\Gamma_{ee} \cdot Br(X \to \gamma\gamma, hadrons, ee, \mu\mu)$.

Table 4: 95% C.L. limit for the case of broad resonance, assuming $M_X = 58$GeV and $\Gamma_{TOT} = 1$GeV.

| | Scalar | Tensor |
|---|---|---|
| $\Gamma_{ee} \cdot Br(X \to \gamma\gamma)$ | < 8.9 keV | < 0.05 keV |
| $\Gamma_{ee} \cdot Br(X \to had)$ | < 11.6 keV | < 2.6 keV |
| $\Gamma_{ee} \cdot Br(X \to ee)$ | < 22.9 keV | < 13.2 keV |
| $\Gamma_{ee} \cdot Br(X \to \mu\mu)$ | < 5.3 keV | < 1.4 keV |

We can set limits on the $\Gamma_{ee} \times$ branching fraction for narrow resonance based on the formula;

$$\int \sigma_{res} dW = (2J+1)\frac{2\pi^2}{m_X^2}\Gamma_{ee} \cdot Br(X \to \gamma\gamma, ..etc.).$$

We assumed flat detector acceptance for scalar particle. For tensor particle, we took calculation by Hagiwara et al.[15] (KEK theory group) for the determination of angular acceptance. Production cross section of tensor particle is simply 5 times of scalar particle except for the $e^+e^-$ final state. In fig.11(b) limits given by TOPAZ[14] are shown. Typically, limit of $\Gamma_{ee} \cdot Br(X \to \gamma\gamma)$ is around 0.3 to 1.0 keV in this region.

In the case of very broad resonance, our limit is somewhat larger, but on the other hand, our sensitive area is extended outside the scanned area due to its broadness. In general, for broad resonance, the limit is a few times larger than the case of narrow resonance (table 4).

Concludingly, no significant evidence has been found in those reactions for hypothetical particle '$X$' suggested by L3, and the measurements are all consistent with the standard model.



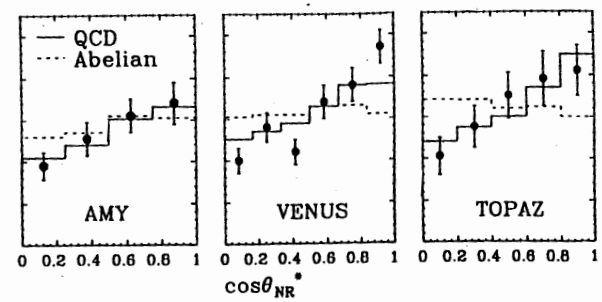


Figure 12: Angular distribution of 4-jet events compared to QCD and Abelian models.

# 4 QCD studies

## 4.1 Gluon self coupling

The triple gluon coupling is a unique property of the non-Abelian nature of QCD. Measurement of the triple coupling was pioneered by AMY group[16] at TRISTAN. Now we have an order of magnitude larger sample of events than that time, we can verify it with much accuracy. The triple gluon coupling is effectively studied by the angular distribution of 4-jet events, extracting the contribution of the radiated gluon splits to two gluons.[17] Several testing quantities are defined by 4 jet momentum vectors $\vec{p}_1, \vec{p}_2, \vec{p}_3, \vec{p}_4$ whose suffix numbers are ordered according to the jet energies. For example, $\theta^*_{NR}$ is the angle between $\vec{p}_1 - \vec{p}_2$ and $\vec{p}_3 - \vec{p}_4$.[18] The results from 3 groups are shown in fig.12 compared with QCD and Abelian models. AMY's pioneering work was confirmed by all groups with higher statistics. From those results, Abelian model is excluded at more than 99% confidence level.

## 4.2 Measurement of $\alpha_s$ with less ambiguity

Perturbative QCD predicts running coupling $\alpha_s$ with momentum transfer $Q^2$. It is important to measure $\alpha_s$ with less uncertainty at different energy, and see how it runs. PEP-4, TOPAZ and ALEPH groups agreed to push a joint analysis program of $\alpha_s$ mearsurement with the same method to explore the energy dependence (PTA collaboration).

It is important to note that the measuring accuracy of $\alpha_s$ is not bound by statistics, but bound by systematic error and theoretical ambiguity. Recently there are several theoretical progresses in calculating $\alpha_s$ from experimental data.

One is NLL (Next to Leading Log) parton shower program by Kato and Munehisa[19] from TRISTAN theory group. Because $\Lambda_{\overline{MS}}$ is arbitrary in Leading Log Approximation, we have to go to Next to Leading Log Approximation in defining $\Lambda_{\overline{MS}}$. Another method is called as 'resummed formula', which analytically calculates various observables up to complete second order $\alpha_s$, and a resummation of the leading and next to leading logarithms to all orders of $\alpha_s$ is done. This was applied to the recent LEP experiments.[20-22]

Here we like to present the analysis done by TOPAZ group[24] which is a typical example of these works in TRISTAN. We obtained $\alpha_s$ from thrust ($T$), heavy jet mass ($\rho = (M^{jet}_{heavy}/E_{vis})^2$) and differential jet rate ($y_3$). $M^{jet}_{heavy}$ is the heavier jet invariant mass in two hemispheres separated by a perpendicular plane to $T$ axis. $y_3$ is defined as the smallest value of jet resolution parameter $y_{ij} = 2[Min(E_i^2, E_j^2)](1 - \cos\theta_{ij})/E^2_{vis}$ which recognizes the three separated jets with Durham jet clustering algorithm.[23] These variables are supposed to be collinear safe, and give close values for parton level and hadron level distribution.

Comparison is done between acceptance corrected experimental data and calculated particle distribution after hadronized and smeared by Monte Carlo (see fig.13). Fit is done in the region where hadron/parton correction is small. Solid histograms show the fit by NLLjet Monte Carlo, and smooth curves show the fit by resummed formula. Best fit values for $\alpha_s$ for each observables and theoretical method are summarised in table 5.

Systematic error in NLLjet method mainly comes from cut off parameter $Q_0$ in the fragmentation model. Main source of the systematic error in the resummed formula are theoretical uncertainty in matching linear or log in the resummation process, and scale parameter dependence which is small but still remains. We have changed $ln(\mu^2/s)$ from $-1$ to 1, and the difference is included in the systematic error.

Comparison of TOPAZ and AMY results with similar method at 58 GeV is given in fig.14. Preliminary result of PTA collaboration at different energies with resummed formula is summarized in fig.15. At this moment, $\Lambda_{\overline{MS}} = 364$ MeV fits well with the results of 3 groups.



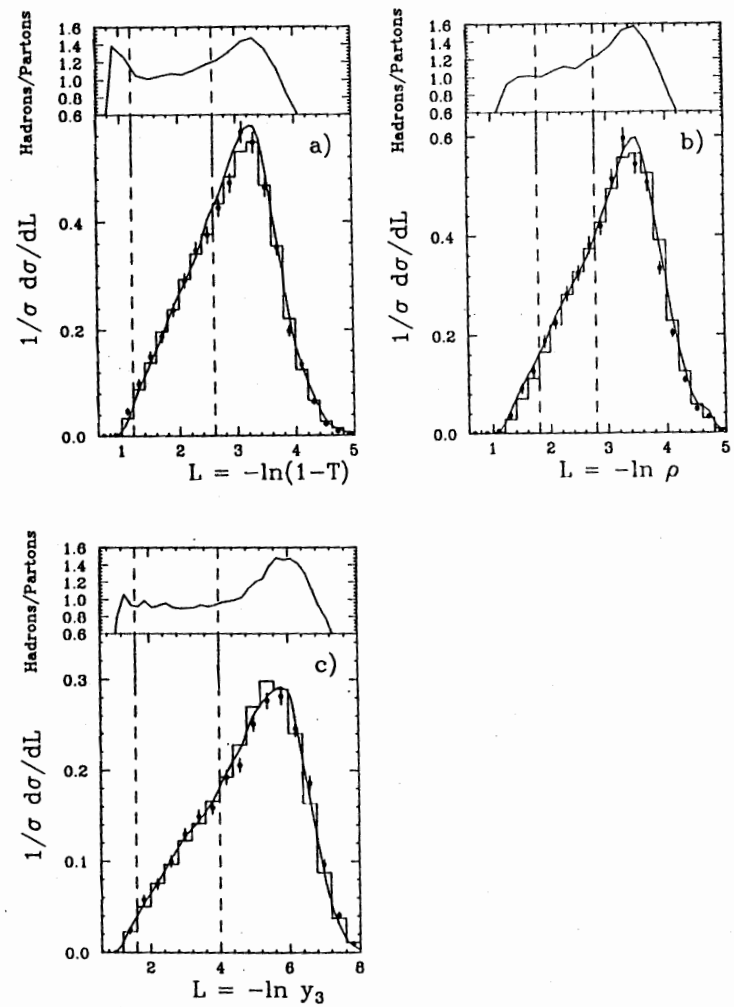


Figure 13: $T, \rho$ and $y_3$ distributions compared to NLLjet (solid histograms) and resummation method (smooth curve) at $E_{CM} = 58$GeV.

Table 5: The fitting results of $\alpha_s$(58GeV) from $T, \rho$ and $y_3$ by NLLjet and resummation method.

| Method | obs. | $\alpha_s$(58GeV) | stat. | exp. | hadr. | theor. |
|---|---|---|---|---|---|---|
| NLLjet | $T$ | 0.1249 | ±0.0050 | ±0.0012 | ±0.0035 | ±0.0029 |
| | $\rho$ | 0.1235 | ±0.0059 | ±0.0006 | ±0.0013 | ±0.0036 |
| | $y_3$ | 0.1309 | ±0.0050 | ±0.0024 | ±0.0026 | ±0.0103 |
| resum. | $T$ | 0.1339 | ±0.0040 | ±0.0008 | ±0.0022 | $^{+0.0070}_{-0.0059}$ |
| | $\rho$ | 0.1287 | ±0.0041 | ±0.0005 | ±0.0020 | $^{+0.0057}_{-0.0046}$ |
| | $y_3$ | 0.1322 | ±0.0056 | ±0.0025 | ±0.0010 | $^{+0.0055}_{-0.0041}$ |

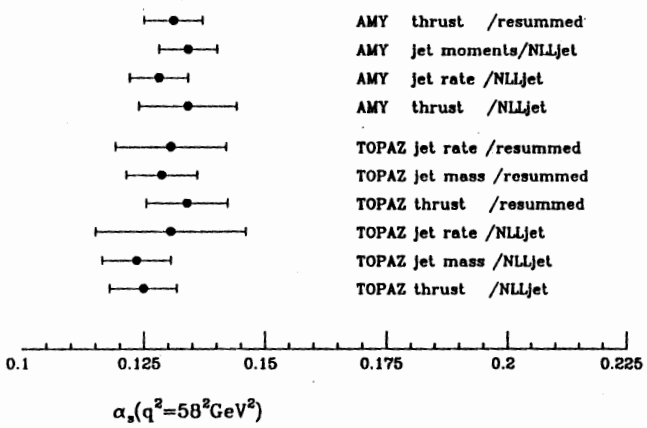


Figure 14: Comparison of $\alpha_s$ value measured by TOPAZ and AMY with several different methods.



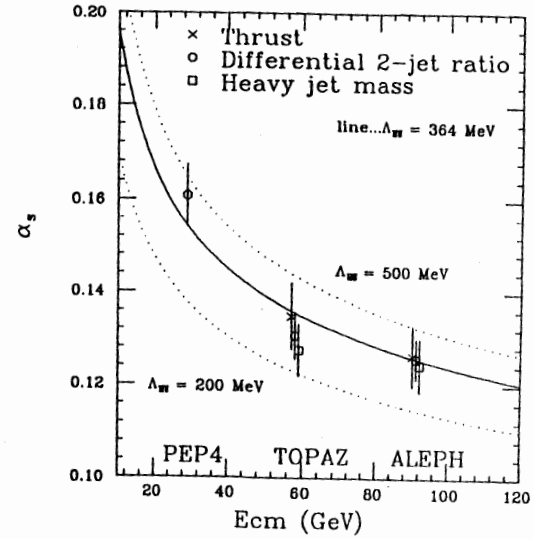


Figure 15: Preliminary result on $E_{CM}$ dependence of $\alpha_s$ by PTA collaboration.

## 4.3 Property of gluon jet

In QCD, gluons have larger color charge than quarks. According to the Altarelli-Parisi[25] splitting kernels, the ratio of gluon to quark bremsstrahlung probability is roughly 9/4. Therefore, gluon jet is expected to have higher multiplicity, and consequently has softer particle distribution than a quark jet.

VENUS group[26] tried to derive the particle spectra for gluon jets by comparing the spectra of two types of event sample; (i) three-fold symmetric ('Mercedes like') 3 jet events ($qqg$ sample), and (ii) three-fold symmetric 2 jets + $\gamma$ events ($qq(\gamma)$ sample), where $\gamma$ was emitted by initial state radiation towards the beam pipe and undetected. Since the two quark jets in the $qqg$ sample are identical to the $qq(\gamma)$ sample topology, definite comparison between gluon jet and quark jet is possible in the same detector and the same kinematical condition.

Common requirements to the 3-jet and 2-jet + $\gamma$ sample is that the total energy should be larger than 5 GeV, no hard $\gamma$ emittion in the active region of the detector, 3 angles between jets (or $\gamma$) are in between 100° and 140°, and total of these angles is larger than 358°. For $qqg$ candidate, visible energy should be

larger than 1/2 of collision energy and momentum should be balanced. For $qq(\gamma)$ candidate, visible energy should be more than 1/3 of collision energy, and requires momentum balance should be between 0.3 and 0.7, which means $\gamma$ escapes in the beam pipe. After those selections are done, averaged jet energy is around 19 GeV for both candidates.

In $qq(\gamma)$ sample, jets are supposed to be purely quark jet. On the other hand, in $qqg$ sample, 1/3 of jets are from gluon and 2/3 are from quark. For each sample, fractional momentum ($x_p$) distribution of the charged particles are plotted in fig.16(a). Significant deviation can be observed between two distributions. The contribution from the gluon jets can be extracted by a waighted subtraction of $q\bar{q}(\gamma)$ sample from $qqg$ sample as shown in fig.16(b). Assuming $qq(\gamma)$ sample to be a purely quark jet, we can clearly see that gluon jet is significantly softer than quark jet.

Another way to present the difference is to calculate the following ratio $R(x_p)$;

$$R(x_p) = \frac{1}{3}\frac{1}{\sigma^{tot}_{qqg}}\frac{d\sigma(qqg)}{x_p} \Big/ \frac{1}{2}\frac{1}{\sigma^{tot}_{qq(\gamma)}}\frac{d\sigma(qq(\gamma))}{x_p}.$$

This ratio is plotted in fig.17 together with the prediction of the various Monte Carlo models. Again it shows that the gluon jets are softer than the quark jets, and also that the parton shower model agrees well with the experiment.

# 5 Two photon process

## 5.1 Inclusive jet production

It has been known[27,28] that the hadron production in $\gamma\gamma$ process is not completely explained by Vector Dominance Model (VDM) and Quark Parton Model (QPM). Drees et al.[29] mentioned that hadronic component of $\gamma$ plays an important role in hadron production in the high energy $\gamma\gamma$ processes, and multi-jet events are expected (fig.18). In resolved photon processes shown in fig.18, one or two spectator jets are produced predominantly along the beam direction. Those events will provide us information on gluon density in the photon as well as quark density, which are ambiguous at present and several models give quite different distribution functions especially for gluons (fig.19). TRISTAN energy region starts to be dominated by hard scattering of photons.



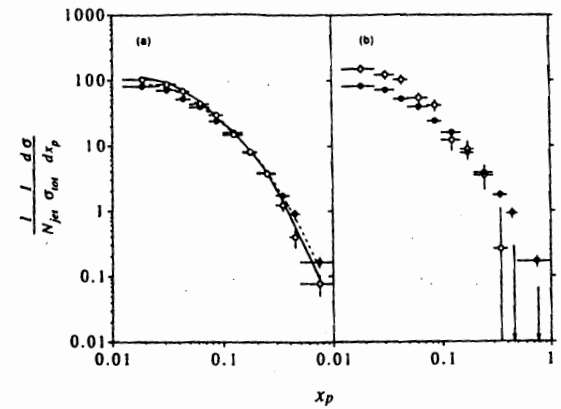


Figure 16: (a) $x_p$ distributions for $qqg$ (open circles) and $qq(\gamma)$ (solid circles) sample. The prediction of the PS model are shown with a solid (dashed) curve for $qqg$ ($qq(\gamma)$) sample. (b) The extracted $x_p$ distributions for gluon jets (open circles) and for quark jets (solid circles).

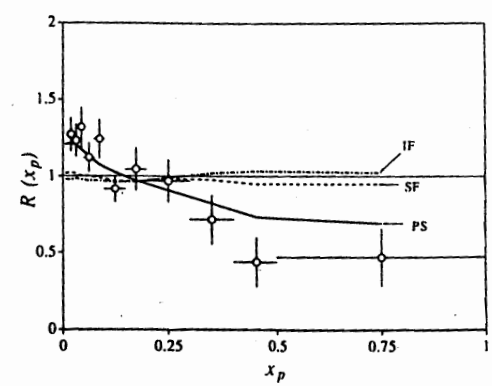


Figure 17: The ratio $R(x_p)$ v.s. $x_p$ together with several model predictions.

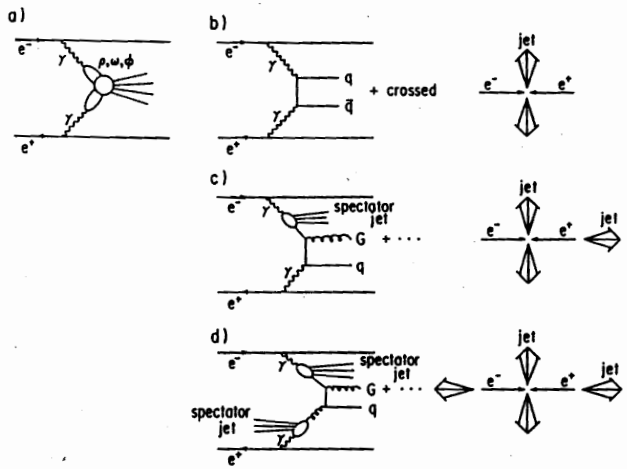


Figure 18: Diagrams and the final state event topology for (a) the VDM, (b) the QPM (direct), and examples of (c) single resolved and (d) double resolved processes.

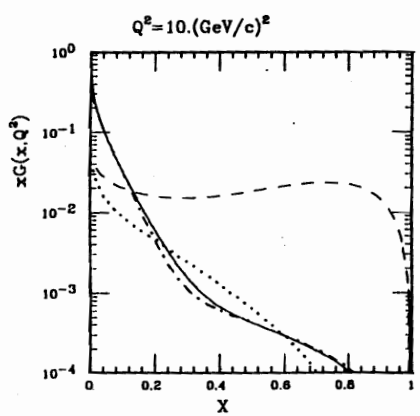


Figure 19: Comparison of the gluon distribution function in the photon by various for the DG and LAC1, LAC2 and LAC3 models at $Q^2 = 10(\mathrm{GeV/c})^2$. The solid, dott-dashed, dashed and dotted curves represent the LAC1, LAC2, LAC3 and DG models, respectively.



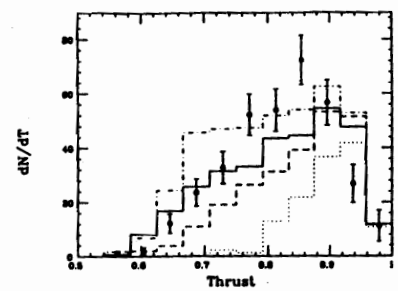


Figure 20: Thrust distribution for the events with $P_T^{jet} > 3\mathrm{GeV/c}$, compared with (i) VDM+QPM (dotted), (ii) VDM+QPM+MJET (solid) for DG parton density with $P_T^{min}$=1.6GeV/c, (iii) VDM+QPM+MJET (dot-dashed) for DO with $P_T^{min}$=2.4GeV/c, and (iv) VDM+QPM+MJET (dashed) with no gluon contribution.

AMY group[30] demonstrated the hard scattering of photons in thrust distribution from notag $\gamma\gamma$ events with $p_T^{jet} > 3\mathrm{GeV/c}$, which is compared with VDM, QPM, and Multi-JET (MJET) model with and without taking care of gluon content of the photon (fig.20). Contribution of MJET with gluon is evident.

TOPAZ group[31] tried to define a jet as a cluster comprising particles inside a unit circle on pseudorapidity ($\eta \equiv -\ln\tan(\theta/2)$) and azimuthal angle ($\phi$) plane. Particle $i$ is included in a jet $J$ if $(\eta_i - \eta_J)^2 + (\phi_i - \phi_J)^2 < 1$. This jet clustering method has been used for hadron collider experiments, which is also suitable for this case since a high $p_T$ jet ($p_T^{jet} > 2.5\mathrm{GeV/c}$ in this case) can be well separated from the remnant spectator jets in the $\eta - \phi$ plane. A typical 2-jet event is shown in fig.21.

To make direct quantitative comparison with theoretical prediction, jet inclusive cross sections are defined as follows;

$$\frac{d\sigma(1jet)}{dp_t} \equiv \int_{-0.7}^{+0.7} d\eta_1 \int_{all} d\eta_2 \frac{d\sigma}{d\eta_1 d\eta_2 dp_t}$$

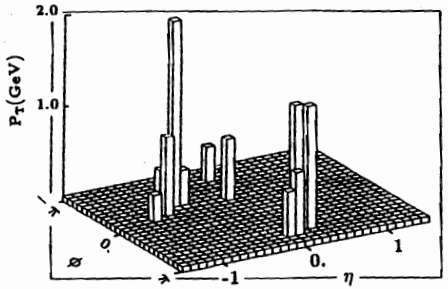


Figure 21: Lego plot of the typical 2-jet event in the $\eta - \phi$ plane.

for $e^-e^+ \to e^-e^+ + jet + X$, and

$$\frac{d\sigma(2jets)}{dp_t} \equiv \int_{-0.7}^{+0.7} d\eta_1 \int_{-0.7}^{+0.7} d\eta_2 \frac{d\sigma}{d\eta_1 d\eta_2 dp_t}$$

for $e^-e^+ \to e^-e^+ + jet + jet + X$. In fig.22, inclusive one jet and two jet cross section as a function of $p_T^{jet}$ for the pseudorapidity interval $|\eta| < 0.7$ are compared with direct only process (VDM+QPM) and various hard scatteing model with different assumptions on gluon density distribution (fig.19). In the two-photon process, $p_T$ distribution is sensitive to parton distribution at relatively larger $x$ region ($x > 0.1$). This is complementary to the $ep$ collision experiment at HERA which is sensitive to very small $x$ region, say $x < 0.02$. From comparison with the data, LAC3,[32] D0[33]+VMD and DG without gluon[34] contribution are excluded and DG with gluon,[34] LAC1 and LAC2[32] are acceptable. Detailed information on the gluon density distribution in the photon will be revealed by further study of $\gamma\gamma$ hard scattering processes.

## 5.2 $c\bar{c}$ production in two-photon collision

$c\bar{c}$ production in $\gamma\gamma$ process also provide us information on parton distribution in the photon (fig.23).

VENUS tried this by inclusive $e^-$ detection with lead glass Cerenkov counter and transition radiation detector, and obtained 93 candidate events in the kinemtical region of $0.8 < p < 4.0$GeV/c and $|\cos\theta| < 0.68$. Background subtraction were done by two different methods, (i) using vetex chamber information and (ii) us-



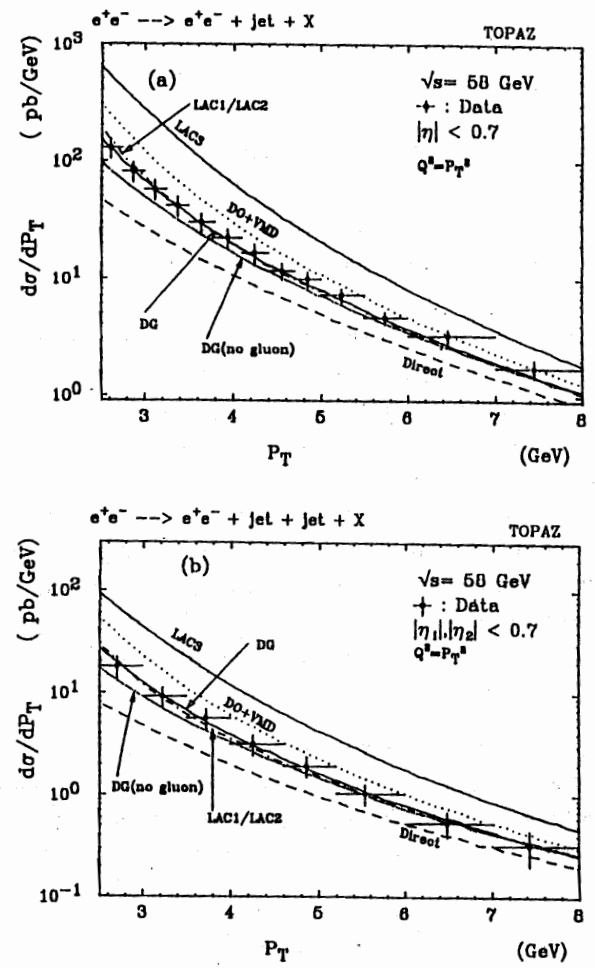


Figure 22: Inclusive (a) one jet, and (b) two jet cross section as a function of the jet transverse momentum. Data are compared with DG (with and without gluon), LAC1, LAC2, LAC3 and DO+VMD.

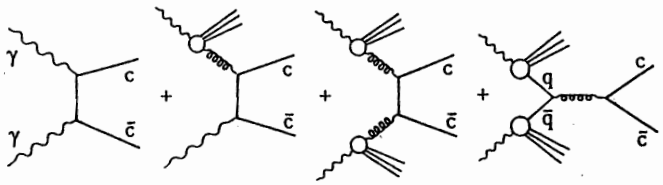


Figure 23: Charm pair prodction mechanism in $\gamma\gamma$ collision.

ing impact parameter distribution, which give $50.0 \pm 11.7$ events and $41.9 \pm 12.5$ ebvents, respectively. Both are 2~3 times larger than the calculation by VDM + QPM + 1 resolved processes, which gives $16.7 \pm 1.3$ events.

Another method is to identify $D^*$ by mass difference method $\Delta M = M_D^* - M_D$ in various exclusive decay channels[35] (fig.24(a)). Cross section is plotted in fig.24(b) together with prediction by QVM + QPM + MJET model with reasonable assumption of gluon density. Cross section for $2.6 < p_t < 6.4$ GeV is $19.8 \pm 7.0$ pb, which is about as twice as the expected value 9.0 pb. This is an excess of more than 10 pb, and parametrization in the resolved process, which is most ambiguous at this moment, can count for 2~ 3 pb, but this excess is much more than that.

There are still large ambiguity in calculating QCD processes in the two photon collision, and the apparent excess of charm events could be explained by those effects. If QCD processes are not enough to fill the gap, we may have to consider some new process, for example, production of light scalar top with mass around 15~25 GeV, which dominantly decays to $c + \tilde{Z}_1$. This excess should be checked further at various final states and with much high statistics.

## 6 Summary and Future Prospects

Test of electroweak theory in $\gamma - Z$ interference region was improved in both lepton and quark sectors. Heavy neutral boson suggested by L3 data was searched in the mass range of 58~60 GeV. No anomalous signal was observed, leading to limits on partial decay width.



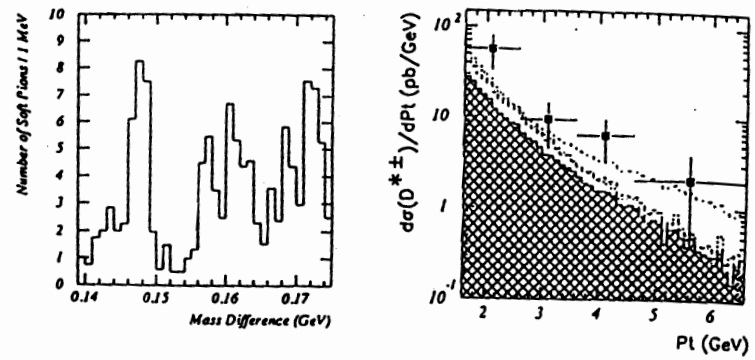


Figure 24: (a) Mass difference $\Delta M = M_D^* - M_D$ shows $D^*$ signal in two photon process. (b) Differential cross section $d\sigma(D^{*\pm})/dp_t$.

Triple gluon coupling was established. Strong coupling $\alpha_s$ was measured by several observables in the theoretical framework with less uncertainty. Running nature of $\alpha_s$ was tested in comparison with PEP and LEP data. Significant difference was observed in $x_p$ spectrum for 3-fold symmetric $qqg$ and $qq(\gamma)$ sample, implying gluon jets were softer than quark jets.

Hard scattering of photons was confirmed in $\gamma\gamma$ processes, wich carriy informations on quark/gluon distribution in the photon. Excess of $c\bar{c}$ production in $2\gamma$ process were seen, which could be attributed to QCD effect still having large uncertainty or some new physics.

More precise results with high integrated luminosity will extend our search area for compositeness and $Z'$. Also precision test of QED will be made in $e^+e^- \to e^+e^-$ and $\gamma\gamma$ processes. Joint PTA collaboration will cover much more subjects such as soft QCD and two photon physics. In two photon prcesses, we will have better understanding of quark/gluon distribution in the photon. We also need this knowledge to reveal what is happening in $c\bar{c}$ production in the $\gamma\gamma$ process.

Results with $\int Ldt \geq 300pb^{-1}$ will be available soon, and we hope this will allow us to have deeper understanding on these subjects.

## References


[1] Particle data group, Phys. Rev. D45 (1992) IX.12

[2] Topaz Collab., I. Adachi et al., Phys. Lett. 234B (1990) 525, Phys. Lett. 255B (1991) 613

[3] VENUS Collab., K. Abe et al., Phys. Lett. 246B (1990) 297, Phys. Lett. 234B (1990) 382, Z. Phys. 48C (1990) 13; H. Yoshida et al., Phys. Lett. 198B (1987) 570

[4] AMY Collab., T. Kumita et al., Phys. Rev. D42 (1990) 1339,; T. Mori et al., Phys. Lett. 218B (1989) 499; A. Bacala et al., Phys. Lett. 198B (1989) 112

[5] Particle data group, Phys. Rev. D45 (1992) V.14

[6] CDF Collab., F. Abe et al., Phys. Rev. Lett. 68 (1992) 1463

[7] S. Jadach et al., Comp. Phys. Comm. 66 (1991) 276

[8] VENUS Collab., F. Hinode et al., Phys. Lett. 313B (1993) 245

[9] TOPAZ Collab., E. Nakano et al., Phys. Lett. 314B (1993) 471

[10] AMY Collab., LiYu Zheng et al., Proceedings of the Workshop on TRISTAN Physics at High Luminosity p.265, KEK Proceedings 93-2

[11] L3 Collab., O. Adriani et al., Phys. Lett. 295B (1992) 337

[12] VENUS Collab., K. Abe et al., Phys. Lett. 302B (1993) 119

[13] AMY Collab., K. L. Sterner et al., Phys. Lett. 303B (1993) 385

[14] TOPAZ Collab., K. Abe et al., Phys. Lett. 304B (1993) 373

[15] K. Hagiwara et al., KEK Preprint 92-202

[16] AMY Collab., I. H. Park et al., Phys. Rev. Lett. 62 (1989) 423

[17] M. Bengtsson and P. Zerwas, Phys. lett. 208B (1988) 306

[18] O. Nachtmann and A. Reiter, Z. Phys. 16C (1982) 45

[19] K. Kato and T. Munehisa, Phys. Rev. D39 (1989) 156, Comp. Phys. Comm. 64 (1991) 67

[20] L3 Collab., O. Adriani et al., Phys. Lett. 284B (1992) 471

[21] ALEPH Collab., D. Decamp et al., Phys. Lett. 284B (1992) 163





[22] OPAL Collab., P. D. Acton et al., Z. Phys. C55 (1991) 1

[23] S. Catani, Yu. L. Dokshitzer, M. Olsson, G. Turrock and B. W. Webber, Phys. Lett. 269B (1991) 432

[24] TOPAZ Collab., Y. Ohnish et al., Phys. Lett. 313B (1993) 475

[25] G. Altareli and G. Parisi, Nucl. Phys. B126 (1977) 298

[26] VENUS Collab., H. Takaki et al., Phys. Rev. Lett. 71 (1993) 38

[27] PLUTO Collab., Ch. Berger et al., Z. Phys. C33 (1987) 351

[28] TPC/2$\gamma$ Collab., H. Aihara et al., Phys. Rev. D41 (1990) 2667

[29] M. Drees and R. H. Godbole, Nucl. Phys. B339 (1990) 355

[30] AMY Collab., R. Tanaka et al., Phys. Lett. 277B (1992) 215

[31] TOPAZ Collab., H. Hayashii et al., Phys. Lett. 314B (1993) 149

[32] A. Ley, H. Abramwics and K. Charchula, Phys. Lett. 269B (1991) 458

[33] D. W. Duke and J. F. Owens, Phys. Rev. D26 (1982) 1600

[34] M. Drees and K. Grassie, Z. Phys. C28 (1985) 451

[35] TOPAZ Collab., R. Enomoto et al., KEK Preprint 93-107